



**HAL**  
open science

## **Emergence of Orai3 activity during cardiac hypertrophy**

Youakim Saliba, Mathilde Keck, Alexandre Marchand, Fabrice Atassi, Aude Ouillé, Olivier Cazorla, Mohamed Trebak, Catherine Pavoine, Alain Lacampagne, Jean-Sébastien Hulot, et al.

► **To cite this version:**

Youakim Saliba, Mathilde Keck, Alexandre Marchand, Fabrice Atassi, Aude Ouillé, et al.. Emergence of Orai3 activity during cardiac hypertrophy. *Cardiovascular Research*, 2015, 105 (3), pp.248 - 259. 10.1093/cvr/cvu207 . hal-01759137

**HAL Id: hal-01759137**

**<https://hal.umontpellier.fr/hal-01759137>**

Submitted on 13 Jun 2021

**HAL** is a multi-disciplinary open access archive for the deposit and dissemination of scientific research documents, whether they are published or not. The documents may come from teaching and research institutions in France or abroad, or from public or private research centers.

L'archive ouverte pluridisciplinaire **HAL**, est destinée au dépôt et à la diffusion de documents scientifiques de niveau recherche, publiés ou non, émanant des établissements d'enseignement et de recherche français ou étrangers, des laboratoires publics ou privés.



# Emergence of Orai3 activity during cardiac hypertrophy

Youakim Saliba<sup>1,2,3</sup>, Mathilde Keck<sup>1,2</sup>, Alexandre Marchand<sup>1,2</sup>, Fabrice Atassi<sup>1,2</sup>, Aude Ouillé<sup>4</sup>, Olivier Cazorla<sup>4</sup>, Mohamed Trebak<sup>5</sup>, Catherine Pavoine<sup>1,2</sup>, Alain Lacampagne<sup>4</sup>, Jean-Sébastien Hulot<sup>1,2,6</sup>, Nassim Farès<sup>3</sup>, Jérémy Fauconnier<sup>4†</sup> and Anne-Marie Lompré<sup>1,2†\*</sup>

<sup>1</sup>Sorbonne Universités, UPMC Univ Paris 06, UMR\_S 1166, ICAN, F-75005 Paris, France; <sup>2</sup>INSERM, UMR\_S 1166, ICAN, F-75005 Paris, France; <sup>3</sup>Laboratoire de Recherche en Physiologie et Physiopathologie, Pôle Technologie Santé, Faculté de Médecine, Université Saint Joseph, Beyrouth, Lebanon; <sup>4</sup>Université Montpellier 1 et 2, Inserm U1046, Montpellier, France; <sup>5</sup>SUNY College of Nanoscale Science and Engineering, Albany, NY, USA; and <sup>6</sup>Cardiovascular Research Center, Icahn School of Medicine at Mount Sinai, New York, NY, USA

Received 15 January 2014; revised 12 August 2014; accepted 3 September 2014

Time for primary review: 32 days

**Aims** Stromal interaction molecule 1 (STIM1) has been shown to control a calcium ( $\text{Ca}^{2+}$ ) influx pathway that emerges during the hypertrophic remodelling of cardiomyocytes. Our aim was to determine the interaction of Orai1 and Orai3 with STIM1 and their role in the constitutive store-independent and the store-operated, STIM1-dependent,  $\text{Ca}^{2+}$  influx in cardiomyocytes.

**Methods and results** We characterized the expression profile of Orai proteins and their interaction with STIM1 in both normal and hypertrophied adult rat ventricular cardiomyocytes. Orai1 and 3 protein levels were unaltered during the hypertrophic process and both proteins co-immunoprecipitated with STIM1. The level of STIM1 and Orai1 were significantly greater in the macromolecular complex precipitated by the Orai3 antibody in hypertrophied cardiomyocytes. We then used a non-viral method to deliver Cy3-tagged siRNAs *in vivo* to adult ventricular cardiomyocytes and silence Orai channel candidates. Cardiomyocytes were subsequently isolated then the voltage-independent, i.e. store-independent and store-operated  $\text{Ca}^{2+}$  entries were measured on Fura-2 AM loaded Cy3-labelled and control isolated cardiomyocytes. The whole cell patch-clamp technique was used to measure Orai-mediated currents. Specific Orai1 and Orai3 knockdown established Orai3, but not Orai1, as the critical partner of STIM1 carrying these voltage-independent  $\text{Ca}^{2+}$  entries in the adult hypertrophied cardiomyocytes. Orai3 also drove an arachidonic acid-activated inward current.

**Conclusion** Cardiac Orai3 is the essential partner of STIM1 and drives voltage-independent  $\text{Ca}^{2+}$  entries in adult cardiomyocytes. Arachidonic acid-activated currents, which are supported by Orai3, are present in adult cardiomyocytes and increased during hypertrophy.

**Keywords** Cardiac hypertrophy • siRNA • Orai • STIM1 • Calcium

## 1. Introduction

Growing evidence suggests that local  $\text{Ca}^{2+}$  sources, independently of excitation–contraction coupling, control  $\text{Ca}^{2+}$ -dependent gene reprogramming in pathophysiological conditions. Store-operated  $\text{Ca}^{2+}$  entry (SOCE) is a major mechanism to raise intracellular  $\text{Ca}^{2+}$  in nearly all non-excitable cells.<sup>1</sup> Stimulation of cell-surface receptors, coupled with phospholipase C, induces inositol trisphosphate (IP3)-dependent  $\text{Ca}^{2+}$  release from the endoplasmic reticulum (ER). Decrease in ER  $\text{Ca}^{2+}$

content opens voltage-independent  $\text{Ca}^{2+}$  release-activated  $\text{Ca}^{2+}$  (CRAC) channels at the plasma membrane, which have a primary role in refilling the ER. In addition, SOCE regulates gene expression and controls many cell functions, including secretion, proliferation, and cell death.<sup>2</sup> SOCE has been described in neonatal and adult cardiomyocytes after stimulation by angiotensin II and endothelin-1, providing  $\text{Ca}^{2+}$  gradients necessary for nuclear factor of activated T-cells (NFAT) nuclear translocation and gene transcription.<sup>3–6</sup> In 2005, STIM1 was found to localize to the endoplasmic/sarcoplasmic reticulum (ER/SR) membrane

\* Corresponding author. Tel: +331 4077 9681; Fax: +331 4077 9645, Email: anne-marie.lompre@upmc.fr

† These authors contributed equally to this work and are co-senior authors.

and shown to function as a primary mediator of SOCE.<sup>7–10</sup> Initial experiments have supported a model wherein STIM1 senses the ER  $\text{Ca}^{2+}$  depletion and subsequently activates plasmalemmal  $\text{Ca}^{2+}$  entry through CRAC channels formed by Orai1 proteins.<sup>10</sup>

Different groups have identified STIM1 as a key component in promoting cardiomyocyte growth both *in vitro* and *in vivo*.<sup>11–14</sup> Recently, Collins et al.<sup>15</sup> reported that cardiac-specific deletion of STIM1 induces ER stress and mitochondrial disorganization followed by contractile dysfunction and left ventricle dilatation. STIM1-dependent SOCE, although inducible in neonatal cardiomyocytes, was marginal in healthy adult cardiomyocytes but a spontaneous STIM1-dependent current reappeared in hypertrophic adult myocytes.<sup>5,11–14</sup> This voltage-independent current was independent of  $\text{Ca}^{2+}$  depletion from the SR thus representing an alternative store-independent pathway for agonist-activated  $\text{Ca}^{2+}$  entry. Indeed, such store-independent  $\text{Ca}^{2+}$  entries, which can be activated by physiological agonists and are not affected by ER  $\text{Ca}^{2+}$  levels, have emerged in different cell types.<sup>16,17</sup> The identity of the STIM1-dependent store-independent  $\text{Ca}^{2+}$  channels at the plasma membrane of cardiomyocytes remains to be determined.

Herein we demonstrate that STIM1 is recruited to Orai3 in cardiac hypertrophy. We used a non-viral strategy to knockdown *Orai1* and *Orai3* *in vivo* in adult rat heart and establish that Orai3 is responsible for the voltage-independent currents observed in cardiac hypertrophy.

## 2. Methods

An expanded method section is available in the Supplementary material online.

### 2.1 Abdominal aortic banding

Adult male 180 g (25 days) Wistar rats (Janvier, France) were used. The animals were housed at a constant temperature (25°C) and humidity; they were exposed to a 12:12 h light–dark cycle. They were fed ordinary rat chow and had free access to tap water. After at least 1 week of acclimatization, the animals were anaesthetized with an intra-peritoneal injection of ketamine (Parke Davis, France) and xylazine (Bayer, France) (75 and 10 mg/kg, respectively). Anaesthesia was monitored by periodic observation of the respiration and pain response.

Medial abdominal laparotomy was performed and a tantalum clip with an internal opening of 0.58 mm was placed. Sham-operated rats served as controls and were subjected to the same surgical procedure without the clip application. Rats were left for 4 weeks to develop the compensated hypertrophy before siRNA delivery. Global cardiac function analysis was conducted every 2 weeks to assess the level of cardiac hypertrophy. Care of the animals and surgical procedures were performed according to the Directive 2010/63/EU of the European Parliament, which had been approved by the Ministry of Agriculture, France, (authorization for surgery C-75-665-R). The project was submitted to the Ethic Committee and obtained the authorization Ce5/2012/050.

### 2.2 *In vivo* ultrasound-mediated siRNA delivery

The siRNA sequences for Orai1 and 2 and Orai 3 were chosen from<sup>18,19</sup> and validated in our own experimental model. The sequences were: siORAI1: 5'-CAACAGCAAUCCGGAGCUU-3'; siOrai2: 5'GCAUGCACCCGUA CAUCGA3'; siORAI3: 5'-GUUUAUGCCUUUGCCCUA-3'. A mixture of Orai1, Orai2, and Orai3 siRNAs or Orai1 and Orai3 siRNA separately were delivered 4 weeks after abdominal aortic banding (AAB), as previously described.<sup>20</sup> For further details see Supplementary material online.

### 2.3 Cardiomyocyte isolation

At the time of sacrifice, 4–6 days after the siRNAs injections, rats were administered an intra-peritoneal injection of sodium pentobarbital (200 mg/kg, Ceva Sante Animale, France). When the animals were completely non-responsive to toe pinching, a thoracotomy was performed; hearts were harvested and kept in ice-cold low  $\text{Ca}^{2+}$  tyrode solution, followed by rapid cannulation and mounting on the Langendorff apparatus. The hearts were perfused with low  $\text{Ca}^{2+}$  for 5 min and then switched to an enzyme solution (1 mg/mL of collagenase A, Roche Applied Science, France) for 50 min. The two solutions were oxygenated and temperature-controlled (37°C). The ventricles were then chopped delicately and aspirated a few times with a pipette; thereafter, the cell suspension was filtered with a 250  $\mu\text{m}$  filter.  $\text{Ca}^{2+}$  was slowly reintroduced to the cell suspension to a final concentration of 1.8 mM. The low  $\text{Ca}^{2+}$  solution contained 117 mM NaCl, 5.7 mM KCl, 4.4 mM  $\text{NaHCO}_3$ , 1.5 mM  $\text{KH}_2\text{PO}_4$ , 1.7 mM  $\text{MgCl}_2$ , 11.7 mM D-glucose, 10 mM creatine monohydrate, 20 mM taurine, 10 mM HEPES (pH 7.1). The enzyme solution was supplemented with 1 mg/mL of collagenase A (Roche Applied Science, France) and 1 mg/mL of BSA (Sigma, France). All chemicals were from Sigma-France. Rod shaped cardiomyocytes isolated from a minimum of three animals were used per experimental condition.

### 2.4 Co-immunoprecipitation and western blot

Isolated cardiomyocytes from sham or AAB were lysed and samples were then centrifuged at 1000 g for 5 min to remove cell debris. Protein concentration was measured by the Bradford assay (BioRad, France). Proteins (600  $\mu\text{g}$ ) were incubated overnight at 4°C in the presence of the anti-Orai1 (20  $\mu\text{g}$ , Santa Cruz sc-68895), anti-Orai3 (20  $\mu\text{g}$ , ProSci 4215), anti-STIM1 (20  $\mu\text{g}$ , Alomone ACC-063), or a control non-relevant antibody (histone 3, Abcam ab1791), followed by incubation with prewashed A/G agarose beads (50  $\mu\text{L}$ ) at 4°C for 2.5 h. Afterwards, the beads were washed six times with lysis buffer; the proteins were then eluted with 30  $\mu\text{L}$  of 2 $\times$  sample loading buffer plus 30  $\mu\text{L}$  of glycine (pH 2.5) and heated to 70°C for 10 min. Samples (40  $\mu\text{L}$ ) were run on a 10% Nu-PAGE gel, transferred to Hybond-C PVDF membrane, according to the manufacturer's protocol (Amersham Biosciences, GE Healthcare, France). The blot was cut horizontally in three pieces, the upper part was hybridized with anti-STIM1 (1:250, Sigma, S6197), the middle part with anti-Orai1 (1:500, ProSci Inc., 4281) and then anti-GAPDH (1:2500, Cell Signaling, 2118), the lower part with anti-Orai3 (1:500, ProSci Inc 4117). The signals were revealed with a clean blot detection reagent (1:400, Thermo Scientific, 21230) which eliminates detection-interference from both heavy-chain (approx. 50kDa) and light-chain (25kDa) IgG-fragments of antibodies used for the initial immunoprecipitation assay. Signals were detected using the Ettan Dige System. Four to six exposures were obtained for each blot and quantification was performed using the most appropriate ones.

### 2.5 Fura-2 AM calcium imaging

Isolated ventricular cardiomyocytes were seeded on laminin and incubated for 20 min in M199 containing 1  $\mu\text{M}$  Fura2-AM (Molecular Probes, Life Technologies, France). Non-transfected cells or cells transfected with Cy3-tagged siRNA, rhythmically beating in response to MyoPacer, were analysed. Measurements were recorded on a Myocyte Calcium and Contractility Recording System (IonOptix, USA).

Each cell was first paced for a few cycles and  $\text{Ca}^{2+}$  transient was recorded to ensure viability and functionality of the cell. Cells were first incubated in tyrode buffer (1.8 mM  $\text{Ca}^{2+}$ ) to check the stability of basal cytosolic calcium levels and then switched to appropriate store-independent or SOCE  $\text{Ca}^{2+}$ -free buffer. Store-independent buffer contained 1  $\mu\text{M}$  ryanodine, 20  $\mu\text{M}$  Diltiazem, and 135 mM N-methyl D-glucamine (NMDG) instead of  $\text{Na}^+$ . SOCE buffer contained 10 mM caffeine (caf) and 2  $\mu\text{M}$  thapsigargin (Tg). Store-independent  $\text{Ca}^{2+}$  entry or SOCE was then measured upon the addition of 1.8 mM  $\text{Ca}^{2+}$ . Data analysis was performed using the IonWizard (v. 6.1) and SigmaPlot (v. 11.0) software.  $\text{Ca}^{2+}$  entry amplitudes were measured by subtracting the ratio values just before re-adding  $\text{Ca}^{2+}$

from those at the  $\text{Ca}^{2+}$  peak. The rates of  $\text{Ca}^{2+}$  entry were estimated by the slope of increasing Fura-2 fluorescence ratios (changes in ratio/s) after the re-addition of  $\text{Ca}^{2+}$ , calculated between time points corresponding to a 10% and a 90% variation in Fura-2 ratio value (relative to the maximal 100% variation in Fura-2 ratio), in each group.

## 2.6 Electrophysiology

Rat ventricular cardiomyocytes were enzymatically isolated and whole-cell patch-clamp experiments, for recording non-specific cation currents, were performed as previously described.<sup>11</sup> The patch pipette contained a standard  $\text{Cs}^+$ -based solution: 137 mM cesium aspartate, 2 mM  $\text{CsCl}$ , 8 mM  $\text{MgSO}_4$ , 15 mM HEPES, and 5 mM EGTA (adjusted to pH 7.2 with  $\text{CsOH}$ ) and 310 mM mOsm (with D-mannitol). The external solution consisted of 150 mM  $\text{NaCl}$ , 2 mM  $\text{CaCl}_2$ , 1 mM  $\text{MgCl}_2$ , 10 mM HEPES, 10 mM glucose, 20 mM sucrose (adjusted to pH 7.4 with  $\text{NaOH}$ ), and 320 mM mOsm (with D-mannitol). In the *N*-methyl-D-glucamine solution,  $\text{Na}^+$  was replaced with an equimolar amount of *N*-methyl-D-glucamine (adjusted to pH 7.4 with  $\text{HCl}$ ). To block the L-Type  $\text{Ca}^{2+}$  currents, verapamil (10  $\mu\text{M}$ ) was added in the external solution;  $\text{K}^+$  channels were blocked by  $\text{Cs}^+$  in the internal solution;  $\text{Na}^+/\text{K}^+$ -ATPase was inhibited with 200  $\mu\text{M}$  ouabain; the voltage-dependent  $\text{Na}^+$  channel was inactivated with the stimulation protocol. Currents were recorded with an Axopatch 200 A amplifier with a Digidata 1200 interface and analysed with the pCLAMP software. Currents were induced every 5 s by 1 s voltage ramp protocols (from +50 to -120 mV) at a holding potential of -80 mV. As quality controls for the patch-clamp configuration, access resistance was required to stay below 6.5 M $\Omega$  and to be stable throughout the analysis; leak current was also not allowed to exceed 100 pA at -80 mV in the external standard solution (with  $\text{Ca}^{2+}$  and  $\text{Na}^+$ ) for 5 min before switching the solution.

## 2.7 Statistical analysis

Quantitative data are reported as means  $\pm$  SEM. Statistical analysis was performed with the SigmaPlot (v11.0) software. When two conditions were compared, Student's *t*-tests or Mann-Whitney *U* tests were used depending, respectively, on the presence or absence of a normal distribution with equal variances. For the colP experiments, AAB values were normalized to Sham in each blot, and we used a one-sample test, testing if the mean of the AAB group differs from 1. For Fura-2 experiments, Kruskal-Wallis one-way analysis of variance (ANOVA) on ranks tests were performed for multiple comparisons of the values because the normal distribution verified with the Shapiro-Wilk test was not met. *Post hoc* analysis was performed with the Dunn's multiple comparison tests to identify the group differences that accounted for the overall ANOVA results. For patch-clamp analysis, statistically significant differences were assessed with a one-way ANOVA with a Newman-Keuls *post hoc* test when three or more groups were compared. All values with  $P < 0.05$  were considered to be significant.

## 3. Results

### 3.1 Orai1 and Orai3 isoforms are expressed in normal and hypertrophied cardiomyocytes

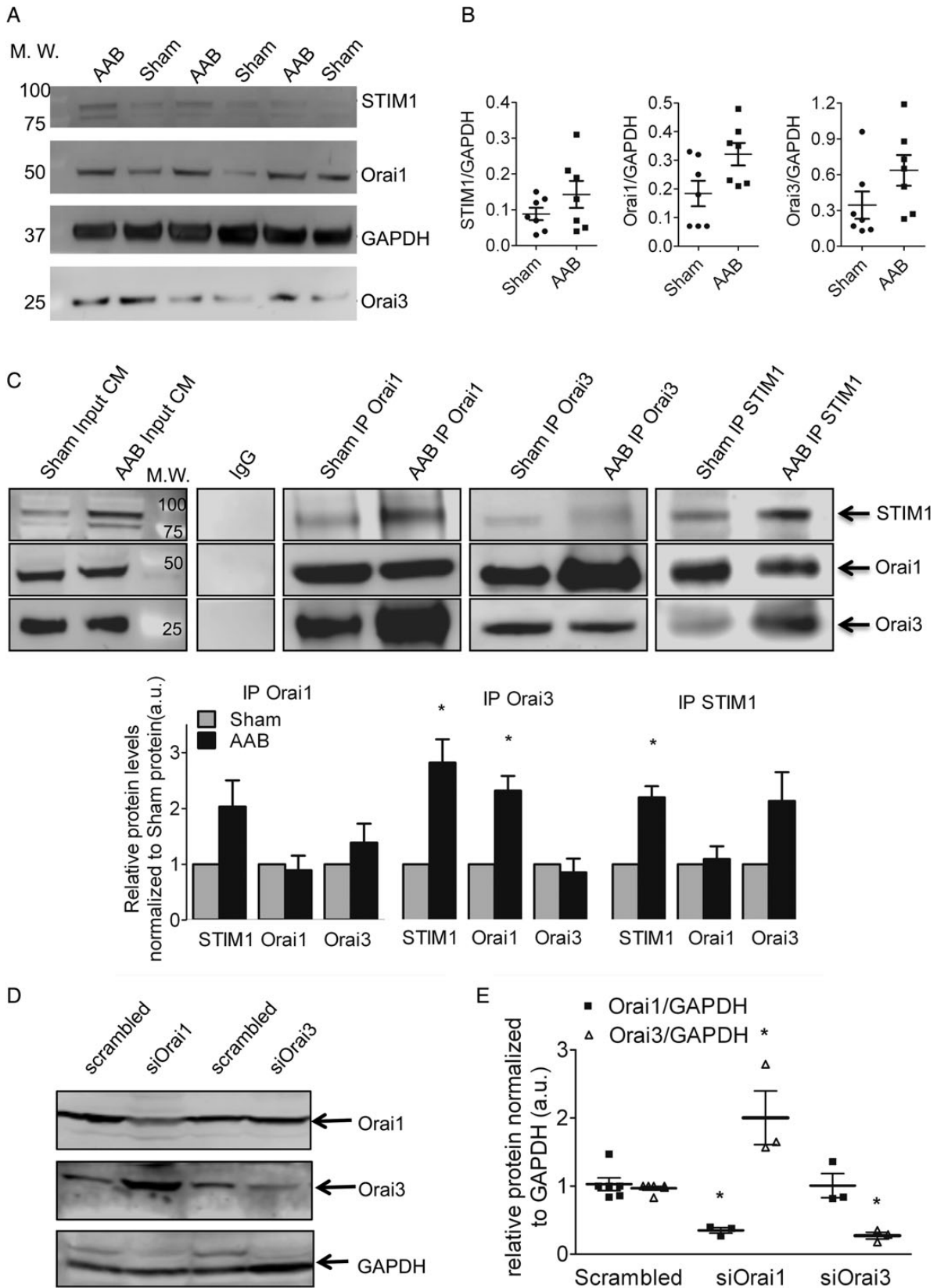
Four weeks after AAB, the heart weight/body weight (HW/BW) ratio was significantly greater in the AAB group. The septum and posterior wall thickness were increased with preserved ejection fraction and fractional shortening that are characteristic of compensated hypertrophy (Table 1). Orai1 mRNA and Orai3 mRNA were detectable in isolated cardiomyocytes but Orai2 mRNA was present at a low level (see Supplementary material online, Figure S1). Orai1 Orai3 and STIM1 proteins were present at variable levels in normal and hypertrophied cardiomyocytes (Figure 1A and B). Despite a similar level of

**Table 1 Echocardiographic cardiac parameters of rats at Day 28 after AAB**

Rat	HR (bpm)	IVSd (mm)	LVd (mm)	PWd (mm)	IVSs (mm)	LVs (mm)	PWs (mm)	EF (%)	FS (%)	HW/BW
Sham (n = 14)	406.68 $\pm$ 17.65	1.44 $\pm$ 0.28	6.56 $\pm$ 0.45	1.4 $\pm$ 0.24	2.26 $\pm$ 0.35	3.9 $\pm$ 0.52	2.4 $\pm$ 0.32	76.84 $\pm$ 4.74	55.2 $\pm$ 3.52	3.5 $\pm$ 0.08
AAB (n = 16)	409.74 $\pm$ 22.01	2.18 $\pm$ 0.22*	7.54 $\pm$ 0.63*	2.24 $\pm$ 0.22*	3.16 $\pm$ 0.21*	4.84 $\pm$ 0.79	2.98 $\pm$ 0.3	71.76 $\pm$ 6.74	54.7 $\pm$ 2.74	5.2 $\pm$ 0.15*

HR, heart rate; IVSd, end-diastolic interventricular septum thickness; LVd, end-diastolic left-ventricular diameter; PWd, end-diastolic posterior wall thickness; IVSs, end-systolic posterior wall thickness; LVs, end-systolic left-ventricular diameter; PWS, end-systolic posterior wall thickness; EF, ejection fraction; FS, fractional shortening; HW/BW, heart weight/body weight ratio. n = 14 and n = 16 for control sham-operated and AAB animals, respectively. Statistical analysis was performed with the Mann-Whitney *U* tests. Data are presented as mean  $\pm$  SEM.

\* $P < 0.05$  vs. sham.



expression in cardiomyocytes from sham-operated and AAB rats, the level of STIM1 and Orai1 were significantly greater in the macromolecular complex precipitated by the Orai3 antibody in lysates from AAB than in lysates from sham cardiomyocytes. Similarly, co-immunoprecipitation with anti-STIM1 suggested an enhanced interaction with Orai3 in AAB (Figure 1C). Thus, it appears that a recruitment of STIM1 to Orai3 occurred in hypertrophied cells.

To further investigate the respective role of Orai1 and Orai3 isoforms in the constitutive  $\text{Ca}^{2+}$  entry, we individually knocked-down *Orai1* and *Orai3* *in vivo* by using non-viral cardiac gene delivery.<sup>20</sup> RT-PCR (see Supplementary material online, Figure S2) as well as western blot from left-ventricular cardiomyocytes demonstrated efficient knockdown of their respective mRNAs and proteins (Figure 1D and E). Notably, there was a compensatory up-regulation of Orai3 protein levels when *Orai1* was silenced, whereas *Orai3* knockdown did not affect Orai1 protein level.

### 3.2 Essential role of Orai3 in store-independent $\text{Ca}^{2+}$ entry in adult normal and hypertrophied cardiomyocytes

To analyse the store-independent  $\text{Ca}^{2+}$  entry, we used a protocol whereby L-type  $\text{Ca}^{2+}$  channels were inhibited by diltiazem (dil, 20  $\mu\text{M}$ ) and ryanodine receptors were blocked by ryanodine (Rya, 1  $\mu\text{M}$ ). Afterwards, a 1.8 mM  $\text{Ca}^{2+}$  solution, in which  $\text{Na}^+$  was replaced by the large organic ion *N*-methyl-D-glucamine (NMDG, 135 mM) to avoid  $\text{Na}^+$  entry via the NCX or  $\text{Na}^+$  channels, was added back. In preliminary experiments, we silenced all three *Orai* (*Orai1–3*) at the same time (Figure 2A). Knockdown of all *Orai* prevented the store-independent  $\text{Ca}^{2+}$  entry in AAB cardiomyocytes demonstrating the essential role of Orai proteins. Next, we silenced either *Orai1* or *Orai3* in sham and AAB cardiomyocytes. The amplitude of store-independent  $\text{Ca}^{2+}$  entry was similar in sham and AAB cardiomyocytes (Figure 2B and C, middle panel). However, the rate of  $\text{Ca}^{2+}$  entry was significantly higher in AAB cells (Figure 2B and C, right panel), indicating a more active entry that is in agreement with the presence of more Orai3 in the STIM1/Orai1/Orai3 complex in these cells. *Orai3* knockdown completely prevented the store-independent  $\text{Ca}^{2+}$  entry in both cell types (Figure 2B). *Orai1* knockdown resulted in significant increases in the amplitude and rate of rise of cytosolic  $\text{Ca}^{2+}$  signal in control and hypertrophied cardiomyocytes (Figure 2C), which is in agreement with the compensatory increase in Orai3 expression in these cells.

### 3.3 Involvement of Orai3 in store-operated $\text{Ca}^{2+}$ entry in adult normal and hypertrophied cardiomyocytes

We next evaluated the presence of store-operated  $\text{Ca}^{2+}$  entry (SOCE) in both transfected and untransfected cells. Experiments were performed in the presence of the L-type  $\text{Ca}^{2+}$  channel inhibitor diltiazem

(Dil, 20  $\mu\text{M}$ ). Caffeine (caf, 10 mM) and thapsigargin (Tg, 2  $\mu\text{M}$ ) were used to deplete intracellular  $\text{Ca}^{2+}$  stores in the absence of added  $\text{Ca}^{2+}$ . For analysis, a 1.8 mM  $\text{Ca}^{2+}$  solution, in which  $\text{Na}^+$  was replaced by NMDG, was added back in order to record the resulting SOCE (Figure 3). Extracellular  $\text{Ca}^{2+}$  re-addition increased fura-2 ratios in a higher amplitude than the ones resulting from the store-independent entry ( $0.82 \pm 0.09$  in sham Tg and  $0.81 \pm 0.14$  in AAB Tg vs.  $0.57 \pm 0.18$  in sham and  $0.5 \pm 0.018$  in AAB;  $P < 0.05$ ). However, the rates of fura-2 rise were slightly but not significantly higher when comparing the two  $\text{Ca}^{2+}$  entries (Figures 2B and 3B). Since Tg did not produce a prominent additional  $\text{Ca}^{2+}$  entry over the store-independent one, these results indicate that the predominant  $\text{Ca}^{2+}$  entry present in adult cardiomyocytes is the store-independent one. In addition, the amplitude of this modest SOCE was similar in AAB and sham cardiomyocytes (Figure 3B and C, middle panel) but the rate of rise of the  $\text{Ca}^{2+}$  signal was greater in AAB myocytes than in sham (Figure 3B and C, right panel). Silencing all three *Orai* in AAB cardiomyocytes completely prevented SOCE (Figure 3A) thereby confirming the role of Orai in this  $\text{Ca}^{2+}$  entry. Specific silencing of *Orai3* (Figure 3B) was sufficient to completely inhibit SOCE in both sham and AAB cardiomyocytes, whereas silencing *Orai1* slightly but significantly increased the amplitude (Figure 3C, middle panel) and rate of rise (Figure 3C, right panel) of the  $\text{Ca}^{2+}$  signal in both sham and AAB cardiomyocytes. Altogether, these results highlight the notion that SOCE in adult cardiomyocytes is a modest contributor for  $\text{Ca}^{2+}$  entry, and Orai3 is involved in the activation of this route.

Finally, we assessed the contribution of these voltage-independent  $\text{Ca}^{2+}$  entries to the  $\text{Ca}^{2+}$  transients in electrically stimulated cells. The rate of rise of the  $\text{Ca}^{2+}$  transient induced by stimulation, as reported by the change in fura-2 ratio, was  $10.7 \pm 0.9 \Delta\text{F}340/\text{F}380.\text{s}^{-1}$  in sham cells and  $11.5 \pm 0.8 \Delta\text{F}340/\text{F}380.\text{s}^{-1}$  in AAB cells. The rates of both voltage-independent  $\text{Ca}^{2+}$  entries ranged between  $0.032 \pm 0.005 \Delta\text{F}340/\text{F}380.\text{s}^{-1}$  for sham cells and  $0.066 \pm 0.006 \Delta\text{F}340/\text{F}380.\text{s}^{-1}$  for AAB cells (Figures 2B and 3B). As previously reported by Huang *et al.*,<sup>21</sup> the rates of voltage-independent  $\text{Ca}^{2+}$  entries were reported to the rates of  $\text{Ca}^{2+}$  transients and were subsequently found to represent  $< 1\%$  of the total transients. These results point out that the store-independent  $\text{Ca}^{2+}$  entry as well as the modest SOCE is not implicated in the fast excitation–contraction coupling in adult cardiomyocytes. To further ascertain this conclusion, silencing *Orai1* or *Orai3* did not affect  $\text{Ca}^{2+}$  transient parameters in electrically stimulated cells (see Supplementary material online, Figure S3).

### 3.4 Orai3 is responsible for voltage-independent $\text{Ca}^{2+}$ entries in cardiomyocytes

We previously showed that during hypertrophy, STIM1 is crucially involved in a SOCE as well as a store-independent current. This

**Figure 1** (A–B) Orai1 and Orai3 are expressed in the normal and hypertrophied rat-ventricular cells. Western blot (A) and quantifications (B) of STIM1, Orai1 and 3 in rat left-ventricular cardiomyocytes, normalized to GAPDH (in arbitrary units, a.u.),  $n = 7$  sham,  $n = 7$  AAB animals. Data are represented as mean  $\pm$  SEM. Comparison between sham and AAB was performed with the Mann–Whitney *U* test. (C) STIM1, Orai1, and Orai3 are present in the same macromolecular complex from sham and AAB cardiomyocytes and a large recruitment of Orai3 occurs in AAB cells. Co-immunoprecipitation of Orai1, Orai3, or STIM1 with STIM1, Orai1, and Orai3 in left-ventricular cardiomyocytes derived from sham-operated or AAB rats. Each co-immunoprecipitation was repeated with extracts from three Sham and three AAB rats. AAB values were normalized to Sham for each blot. Below is the quantification of the western blot. Statistical analysis was performed using a one-sample test, testing if the mean of the AAB group differs from 1: \* $P < 0.05$ . (D and E) Orai3 compensates for the loss of Orai1. Western blot (D) showing the efficient knockdown of Orai1 and 3 in AAB cardiomyocytes. Histograms in (E) representing relative protein levels normalized to GAPDH ( $n = 3$  animals for each condition). Statistical analysis was performed with the Mann–Whitney *U* test. Data are presented as mean  $\pm$  SEM. \* $P < 0.05$  vs. scrambled.

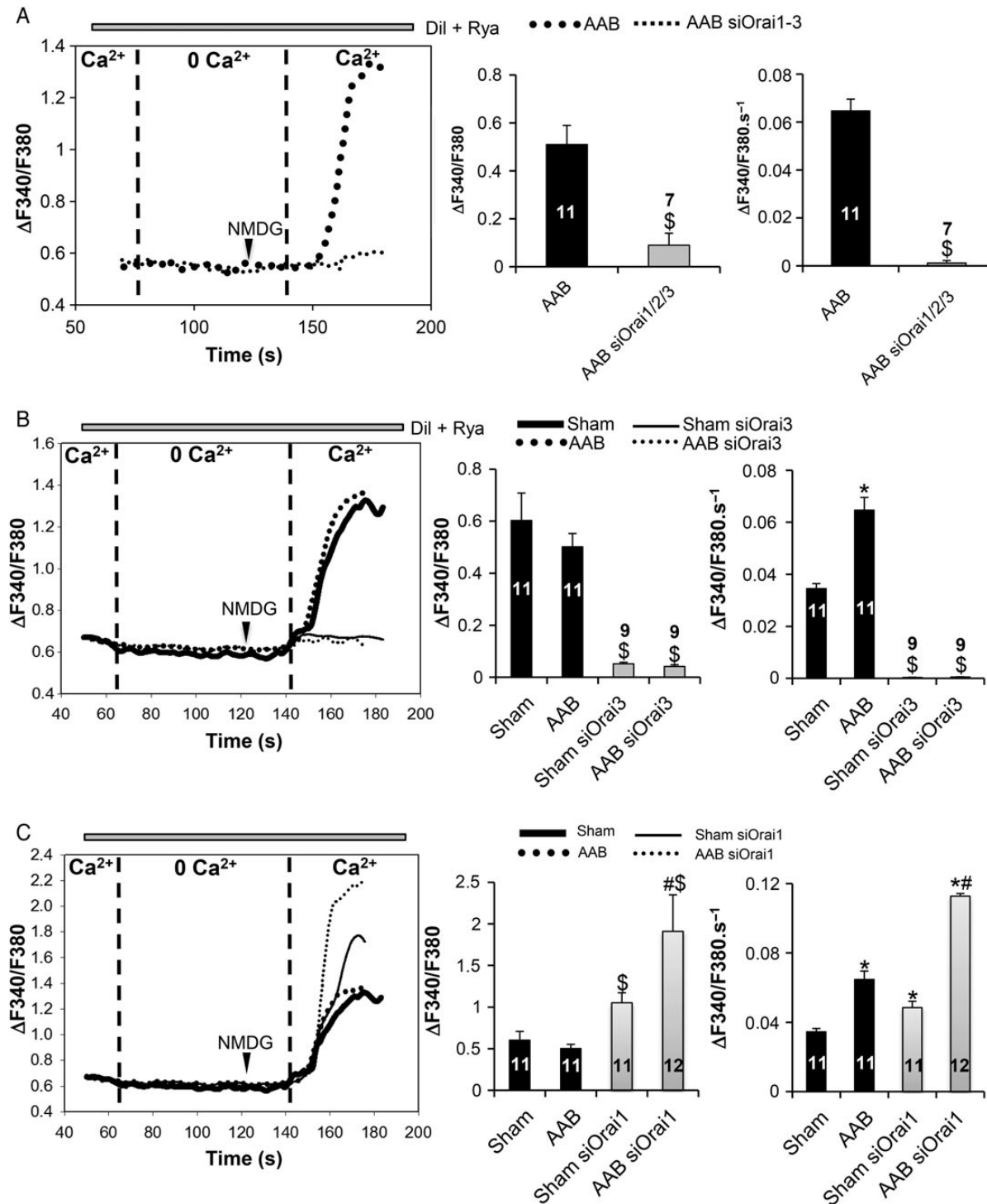


**Figure 2** Effect of Orai knockdown on constitutive  $\text{Ca}^{2+}$  entry. (A and B) Orai1–3 as well as Orai3 knockdown inhibits basal constitutive  $\text{Ca}^{2+}$  entry in left-ventricular cardiomyocytes. Comparison between AAB and AAB siOrai1/2/3 was performed with the Student's *t*-test; while Kruskal–Wallis one-way ANOVA on ranks followed by Dunn's *post hoc* tests were used for the multiple comparisons.  $^{\$}P < 0.05$  vs. sham and AAB, respectively. (C) *Orai1* silencing leads to an increase in basal constitutive  $\text{Ca}^{2+}$  entry. Representative recordings of Fura2 emission ratio ( $\Delta F340/F380$ ) in the cardiomyocytes under basal conditions (left panel). Quantification of the amplitude (middle panel) and the rate of rise (right panel) of the Fura-2 signal in the various conditions. Numbers in the columns represent the number of cells analysed from three different rats for each condition. Statistical analysis was performed with Kruskal–Wallis one-way ANOVA on ranks followed by Dunn's *post hoc* tests. Data are presented as mean  $\pm$  SEM.  $^{\$}P < 0.05$  vs. sham and AAB, respectively,  $^*P < 0.05$  vs. sham,  $^{\#}P < 0.05$  vs. AAB and sham siOrai1.

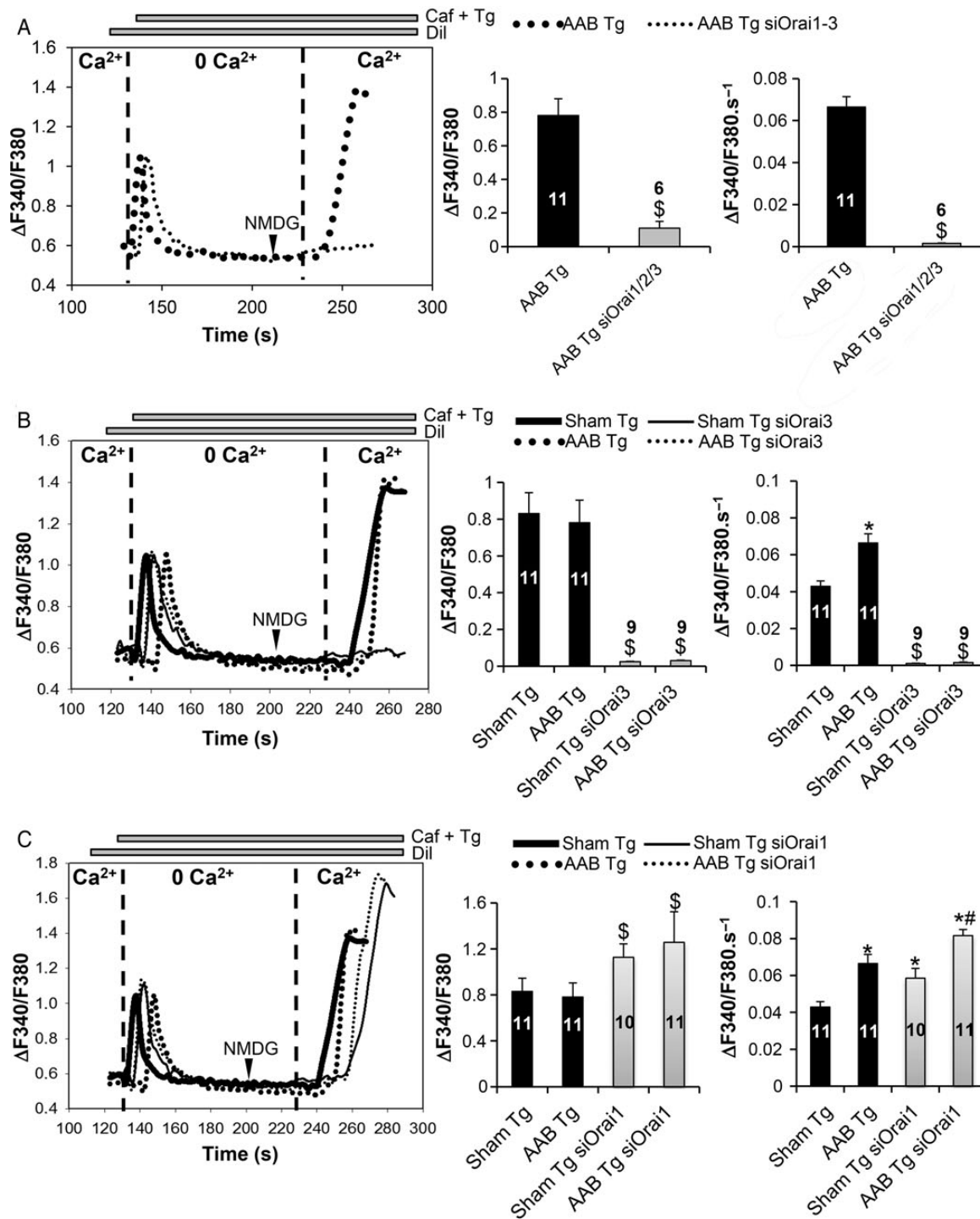


**Figure 3** Effect of Orai knockdown on the store-dependent  $Ca^{2+}$  entry. (A and B) Orai1–3 as well as Orai3 knockdown inhibits SOCE in left-ventricular cardiomyocytes. Comparison between AAB and AAB siOrai1/2/3 was performed with the Student’s *t*-test; while Kruskal–Wallis one-way ANOVA on ranks followed by Dunn’s *post hoc* tests were used for the multiple comparisons.  $^{\$}P < 0.05$  vs. sham Tg and AAB Tg, respectively. (C) *Orai1* silencing leads to an increase in SOCE. Representative recordings of Fura2 emission ratio ( $\Delta F340/F380$ ) in the cardiomyocytes under basal conditions (left panel). Quantification of the amplitude (middle panel) and the rate of rise (right panel) of the Fura-2 signal in the various conditions. Numbers in the columns represent the number of cells analysed from three different rats for each condition. Statistical analysis was performed with Kruskal–Wallis one-way ANOVA on ranks followed by Dunn’s *post hoc* tests. Data are presented as mean  $\pm$  SEM.  $^{\$}P < 0.05$  vs. sham Tg and AAB Tg, respectively,  $^{*}P < 0.05$  vs. sham Tg,  $^{\#}P < 0.05$  vs. AAB Tg and sham Tg siOrai1.



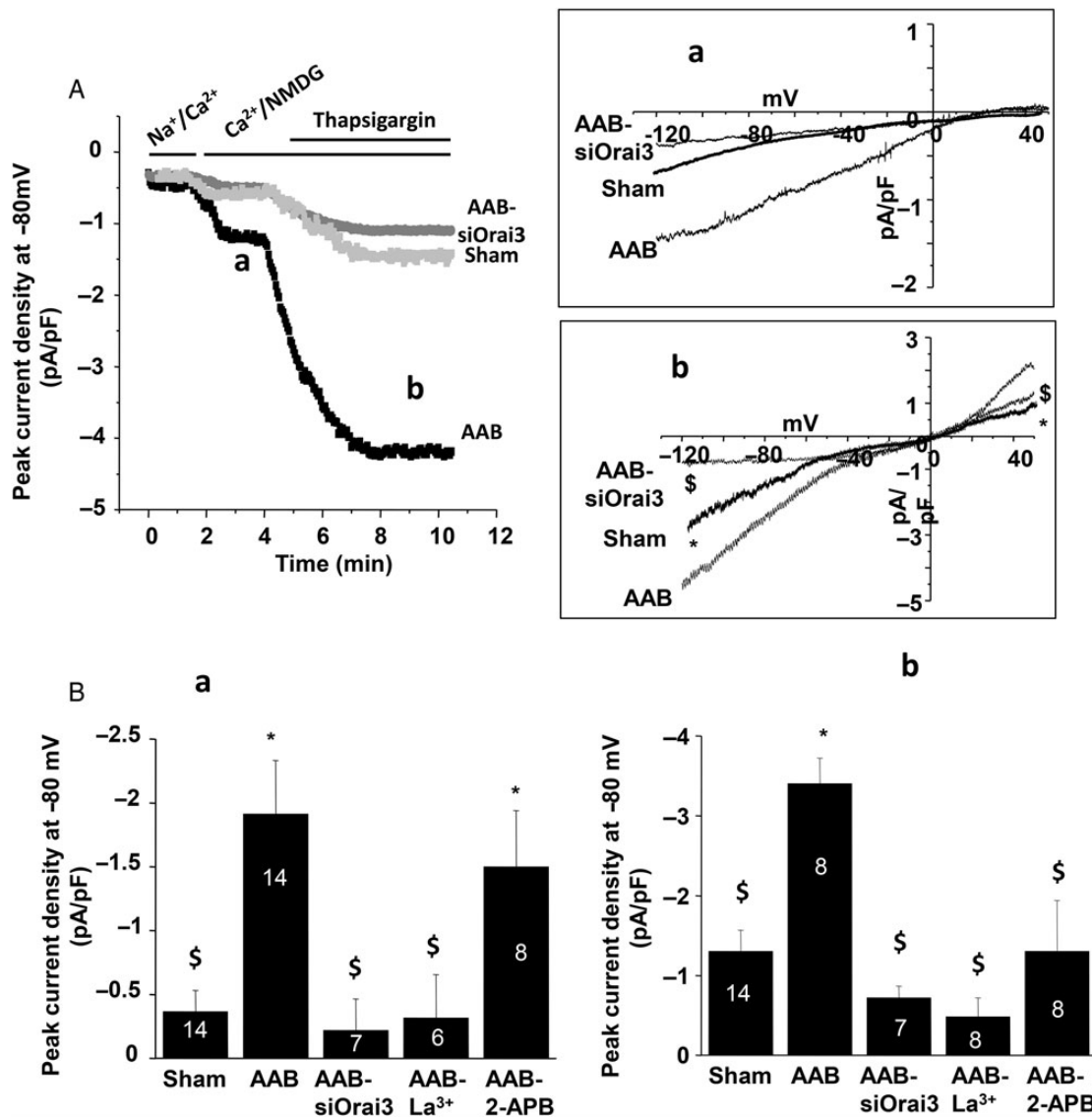


**Figure 4** Orai3-dependent cation currents in adult cardiomyocytes. Whole-cell patch-clamp recordings in ventricular cells. (A) Current density recorded at  $-80$  mV in control cardiomyocytes, hypertrophic cardiomyocytes (AAB), and hypertrophic cardiomyocytes transfected with siOrai3 (AAB+siOrai3). (Aa) Typical current–voltage relationship of a store-independent current revealed by replacing external  $\text{Na}^+$  with NMDG. (Ab) Typical current–voltage relationship of store-dependent current revealed by thapsigargin application obtained after subtraction of the store-independent current (a). (B) Mean values of store-independent (a) and store-dependent (b) peak current density recorded at  $-80$  mV. Mean values in b were calculated on thapsigargin-inducing current after subtraction of the store-independent current. In AAB cardiomyocytes,  $\text{La}^{3+}$  ( $100 \mu\text{M}$ ) or siOrai3 inhibits both the store-independent and store-dependent currents (a), whereas 2-APB addition ( $10 \mu\text{M}$ ) only affects thapsigargin-induced current (b). Numbers in the columns represent the number of cells isolated from three to five rats. Data are presented as mean  $\pm$  SEM. \* $P < 0.05$  compared with sham.  $^{\$}P < 0.05$  compared with non-transfected AAB cardiomyocytes.

store-independent  $\text{Ca}^{2+}$  entry shared electrophysiological, pharmacological, and selectivity properties of Orai.<sup>11</sup> Using the whole-cell patch-clamp technique, we further investigated the role of Orai3 in store-independent and store-dependent currents in adult cardiomyocytes. As previously shown,<sup>11</sup> the store-independent current, revealed by replacing external  $\text{Na}^+$  with NMDG, was greater in rat ventricular hypertrophied AAB cardiomyocytes when compared with sham cardiomyocytes, whereas after *Orai3* silencing in AAB cardiomyocytes, this current was comparable to the one in sham cardiomyocytes (Figure 4Aa and Ba). Furthermore, this current was inhibited by  $\text{La}^{3+}$  but not by 2-APB, supporting the involvement of Orai3 in store-

independent  $\text{Ca}^{2+}$  entry<sup>22</sup> in hypertrophied cardiomyocytes. In addition, as an index of cell surface, the membrane capacitance measured in AAB cardiomyocytes transfected with siOrai3 was significantly reduced when compared with non-transfected AAB cardiomyocytes and comparable to control myocytes ( $241 \pm 8$  pF,  $n = 30$  AAB cardiomyocytes;  $189 \pm 10$  pF,  $n = 14$  sham-operated cardiomyocytes and  $187 \pm 10$  pF,  $n = 7$  AAB siOrai3 cardiomyocytes;  $P < 0.05$  vs. AAB cardiomyocytes). These results indicate that Orai3 plays a critical role in the hypertrophic process of cardiomyocytes.

Following activation of the store-independent current (Figure 4Aa), the store-operated current was further induced by thapsigargin

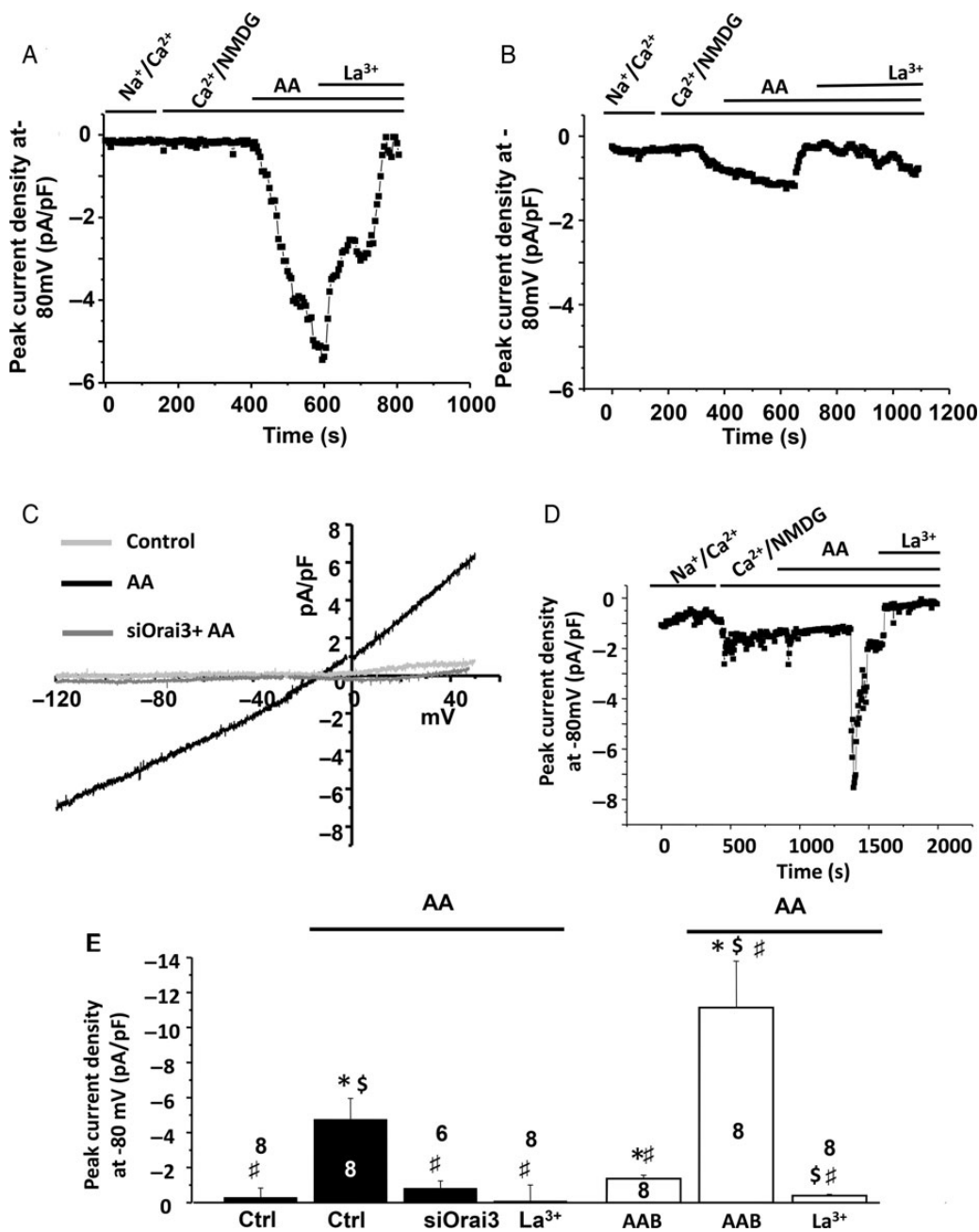


**Figure 5** Orai3 carries an arachidonic acid-inducing current in control and AAB cardiomyocytes. (A) Whole-cell patch-clamp recordings at  $-80$  mV in control adult ventricular cells before and after arachidonic acid (AA;  $8 \mu\text{M}$ ), followed by  $\text{La}^{3+}$  ( $100 \mu\text{M}$ ) external application. (B). Whole-cell patch-clamp recordings at  $-80$  mV in siOrai3 transfected control adult ventricular cells before and after arachidonic acid (AA;  $8 \mu\text{M}$ ), followed by  $\text{La}^{3+}$  ( $100 \mu\text{M}$ ) external application. (C) Typical current–voltage relationship of AA-inducing current obtained in control and transfected adult ventricular cardiomyocytes. Numbers in the columns represent the number of cells isolated from three rats. (D). Whole-cell patch-clamp recordings at  $-80$  mV in adult AAB ventricular cells before and after arachidonic acid (AA;  $8 \mu\text{M}$ ), followed by  $\text{La}^{3+}$  ( $100 \mu\text{M}$ ) external application. (E) Mean values of AA-inducing current recorded at  $-80$  mV in the presence of  $\text{Ca}^{2+}$  and NMDG. Analysis was performed on eight cardiomyocytes isolated from three control animals (ctrl) and four AAB animals. Data are presented as mean  $\pm$  SEM. \* $P < 0.05$  compared with control conditions in the absence of AA.  $^{\#}P < 0.05$  compared with AAB conditions in the absence of AA.  $^{\$}P < 0.05$  ctrl in the presence of AA.

application (Figure 4Ab), and was significantly increased in hypertrophied cardiomyocytes when compared with sham cardiomyocytes. Orai3 silencing in AAB cardiomyocytes markedly reduced the inward component of the SOC current (Figure 4Ab and Bb), arguing for a role of Orai3 channel in the thapsigargin-inducing current. Although this

current was sensitive to  $\text{La}^{3+}$ , 2-APB also partially inhibited it, suggesting that, in addition to Orai3, other channels carry the thapsigargin-inducing current.

Because Orai3 has been shown to mediate arachidonic acid (AA)-induced current (ARC), we then applied AA ( $8 \mu\text{M}$ ) to determine

whether ARC could be triggered in control adult cardiomyocytes and dependent on Orai3. Application of AA activated within 10 min an outward rectifying current relationship with an outward component that contrasted with the store-independent inwardly rectifying current observed in hypertrophied AAB cardiomyocytes (Figure 5A and C). Application of  $\text{La}^{3+}$  (100  $\mu\text{M}$ ) inhibited the AA-activated currents (Figure 5A and E), and AA failed to activate currents in siOrai3-transfected cells (Figure 5B, C, and E) indicating that Orai3 carries an AA-induced current in control cardiomyocytes. In AAB cardiomyocytes, AA application (8  $\mu\text{M}$ ) also activated a current within 10 min that was inhibited by 100  $\mu\text{M}$   $\text{La}^{3+}$  (Figure 5D and E). The AA-induced current was significantly greater in AAB cardiomyocytes when compared with control cardiomyocytes ( $-11.1 \pm 2.7$  pA/pF,  $n = 8$ , vs.  $-4.7 \pm 1.13$ ,  $n = 8$ ,  $P < 0.05$ ; Figure 5E), in agreement with the increased number of STIM/Orai3 complexes.

## 4. Discussion

Our experiments demonstrate that Orai3 plays a major role in the  $\text{Ca}^{2+}$  channel activity that supports the constitutively active STIM1-dependent current, which was previously described in cardiac hypertrophy.<sup>11</sup> Orai1 and Orai3 are both present in adult cardiomyocytes in agreement with previous studies.<sup>23</sup> Despite a similar level of expression in control and hypertrophied cardiomyocytes, there is more Orai1 and STIM1 in the complex precipitated by anti-Orai3 in hypertrophied cells. Thus, the activation of the Orai3-dependent current in hypertrophied cardiomyocytes is likely due to an increased interaction between Orai3/Orai1 and STIM1. This activity and interaction could correspond either to an activation of pre-existing channels by STIM1 or a redistribution of the Orai1 and Orai3 subunits to form new channels. The precise stoichiometry of the CRAC and ARC channels is not yet defined. In the present study, they could correspond to heteromultimers of Orai1 and Orai3 or a mixture of homomultimers of Orai1 and homomultimers of Orai3. Both possibilities could also co-exist. Additional post-translational mechanisms and new regulatory proteins could also modulate STIM1/Orai activity;<sup>24</sup> however, additional studies in the heart during hypertrophy are required to unravel these regulatory mechanisms.

Interestingly, silencing *Orai1* or *Orai3*, in sham or in AAB, does not modify the  $\text{Ca}^{2+}$  transient induced by electrical stimulation, suggesting that  $\text{Ca}^{2+}$  flowing through Orai/STIM1 does not regulate L-Type channels activity and is not involved in adult cardiomyocytes contraction. In contrast, STIM1 or STIM1/Orai1-mediated inhibition of  $\text{Ca}^{2+}$  entry through voltage-gated channels has been reported in excitable neuronal cells, A7r5 vascular smooth muscle cells or T lymphocytes, arguing for a tissue-specific mode of action of STIM1 and Orai1.<sup>25,26</sup> Of note, Wang et al.<sup>26</sup> reported co-localization of Orai and voltage-gated channel proteins within discrete ER/plasma membrane junctions in cells where reciprocal interaction with STIM1 occurs. A peri-junctional SR in close contact with the plasma membrane has also been described in cardiac cells.<sup>27</sup> This region could correspond to the zone of interaction between STIM1 and Orai proteins. The peri-junctional SR is distant from the T-Tubule where the excitation–contraction coupling takes place. In addition, Orai activation kinetics (tens of seconds) compared with action potential-triggered  $\text{Ca}^{2+}$  transients (milliseconds) are much slower and are hardly compatible with an implication of Orai proteins in fast excitation–contraction coupling.

In contrast, our results demonstrate that Orai3 channels play a critical role in the long-term AAB-induced hypertrophic process of

cardiomyocytes. Measurement of capacitance indicates that Orai3 knockdown prevents cardiomyocytes hypertrophy, as previously shown with STIM1 knockdown.<sup>11</sup> Cardiac-specific STIM1 knock-out mice developed with age, independently of induction of pressure overload, progressive decline in cardiac function associated with dilated cardiomyopathy, fibrosis, and premature death.<sup>15</sup> *Orai1*<sup>+/-</sup> mice died prematurely after aortic banding and developed dilated cardiomyopathy.<sup>28</sup> One limitation of our study is that we could not study the role of Orai3 in whole cardiac function; the generation of cardiac-specific Orai3 mice is now necessary to confirm the cardiac pathophysiological role of Orai3.

We show that silencing *Orai1* results in the up-regulation of *Orai3* both in sham and AAB adult cardiomyocytes. Previous studies reported no compensation by *Orai2* or *Orai3* in the heart of *Orai1*<sup>+/-</sup> mice under basal conditions. However, *Orai2* and *Orai3* were up-regulated after thoracic aortic constriction in *Orai1*<sup>+/-</sup> mice but not in WT mice.<sup>28</sup> In neonatal isolated cardiomyocytes, knockdown of *Orai1* was compensated by up-regulation of *Orai2* but not *Orai3*.<sup>14</sup> Although *Orai2* is ubiquitously expressed<sup>29</sup> and present at a low level of expression in the heart (see Supplementary material online, Figure S1), we could not exclude that *Orai2* is functionally relevant in adult ventricular cardiomyocytes. Similarly, in neonatal cardiomyocytes knockdown of *STIM1* was compensated by up-regulation of *STIM2*<sup>14</sup> but cardiac-specific deletion of *STIM1* did not result in the up-regulation of *STIM2*.<sup>15</sup>

In agreement with recent reports documenting interaction between STIM1 and Orai3,<sup>30,31</sup> our results show that Orai3 is recruited to STIM1/Orai1 complexes during AAB-induced compensated cardiac hypertrophy, resulting in an enhanced rate of Orai3-dependent  $\text{Ca}^{2+}$  entries in hypertrophied AAB myocytes. However, the amplitude of Orai3-dependent  $\text{Ca}^{2+}$  entries was similar in myocytes isolated from sham-operated or AAB rats. It likely reflects the fact that the peak of cytosolic  $\text{Ca}^{2+}$  was mainly determined by  $\text{Ca}^{2+}$  affinities of systems ensuring its elimination from the cytosol, i.e. the SR/ER  $\text{Ca}^{2+}$  ATPase or the plasma membrane  $\text{Ca}^{2+}$  ATPase that remained preserved between cardiomyocytes from sham and cardiomyocytes displaying compensated hypertrophy. It also suggests that these systems were still able to efficiently buffer the limited elevation of calcium due to Orai3 currents, despite a possible alteration of maximal velocity with compensated hypertrophy.

In addition to Orai3-driven store-independent  $\text{Ca}^{2+}$  entries, an Orai3-dependent inward component develops upon thapsigargin application in cardiomyocytes. Although SOCE has been generally associated with Orai1,<sup>5,24,32</sup> Orai3 has also been shown to carry SOCE in breast-cancer cells<sup>33,34</sup> and to be an oestrogen receptor-regulated channel.<sup>35</sup> *Orai3* is overexpressed in lung-cancer tissues when compared with the non-tumoral ones, and inhibition or knockdown of *Orai3* significantly reduced SOCE, inhibited cell proliferation, and arrested cells in G0/G1 phase.<sup>36</sup> Similarly, during hypertrophy, the thapsigargin-inducing current is significantly increased (Figure 4<sup>11</sup>), however, the functional relevance of such current on a beat-to-beat basis remains elusive. Of note, our Ca imaging results are mitigated concerning the functionality of SOCE in adult cardiomyocytes, since comparison between store-dependent and store-independent influx protocols only shows a modest difference in the amplitude of Fura-2  $\text{Ca}^{2+}$  signals. This might rely on a possible inhibition of SOCE by store-independent  $\text{Ca}^{2+}$  entries, as previously proposed.<sup>37</sup> But more likely, these results argue for marginal store-operated  $\text{Ca}^{2+}$  entries in adult cardiomyocytes, in accordance with a study by Huang et al.<sup>21</sup> who have used several successive pulses of caffeine to measure SR  $\text{Ca}^{2+}$  reloading via SOCE

and showed that SOCE decreases with age (from 3 to 56 days) in rabbit cardiomyocytes.

We also demonstrate that ARC channels are present in control and hypertrophied cardiomyocytes and that AA-induced inward current is hampered upon *Orai3* knockdown. The current was greater in hypertrophied cardiomyocytes than in control cardiomyocytes, in agreement with more STIM1/*Orai3*/*Orai1* complexes. Interestingly, an elevation in AA in total phospholipids was reported in pressure overload-induced hypertrophy.<sup>38</sup> *Orai3*, the 'exceptional' *Orai*<sup>22</sup> carries a store-independent  $\text{Ca}^{2+}$  entry induced by arachidonic acid (ARC).<sup>39–41</sup> The so-called ARC channel is a small conductance, highly  $\text{Ca}^{2+}$ -selective ion channel whose activation is specifically dependent on low concentrations of arachidonic acid that acts at an intracellular site. ARC channel is thought to be composed by a heteropentamer of *Orai1*/*Orai3*<sup>30,42</sup> and to be dependent on STIM1 for its activation.<sup>16,39</sup> *Orai3* also supports another store-independent entry via a leukotriene C4-regulated  $\text{Ca}^{2+}$  (LRC) channel in vascular smooth muscle cells.<sup>31,43,44</sup> ARC in HEK 293 cells and LRC in vascular smooth muscle cells display similar characteristics; both require *Orai1*, *Orai3*, and STIM1, suggesting that both conductance are mediated by the same channel.<sup>44</sup> We cannot exclude that, in cardiomyocytes, activation of the *Orai3*-dependent, AA-activated, current is also induced by AA metabolites such as leukotriene C4.

Altogether, our results highlight the major role of *Orai3* in myocytes with compensated hypertrophy and point out the need to identify *Orai3* regulatory pathways and downstream effectors in the heart during cardiac hypertrophy.

## Supplementary material

Supplementary material is available at *Cardiovascular Research* online.

## Acknowledgements

We thank Nathalie Mougenot, Adeline Jacquet, and Patrice Bideaux for the AAB and siRNA injection procedures.

**Conflict of interest:** none declared.

## Funding

This study was supported by an ANR (Agence Nationale de la Recherche) grant to A.M.L. and J.F. (Cardiosoc project), and the Research Council of the Saint Joseph University. Y.S. was supported by a Franco-Lebanese contract (Projet Cèdre) and by the French Ministry of Foreign and European Affairs (Egide - Programme Eiffel). M.T. is supported by NIH grants R01HL097111 and R01HL123364, American Heart Association grant 14GRNT18880008, and a visiting professor position from 'la mairie de Paris'; J.S.H. is supported by the NIH grant R01HL113497.

## References

- Putney JW Jr. Identification of cellular activation mechanisms associated with salivary secretion. *Annu Rev Physiol* 1986;**48**:75–88.
- Parekh AB, Penner R. Store depletion and calcium influx. *Physiol Rev* 1997;**77**:901–930.
- Hunton DL, Lucchesi PA, Pang Y, Cheng X, Dell'Italia LJ, Marchase RB. Capacitative calcium entry contributes to nuclear factor of activated T-cells nuclear translocation and hypertrophy in cardiomyocytes. *J Biol Chem* 2002;**277**:14266–14273.
- Hunton DL, Zou L, Pang Y, Marchase RB. Adult rat cardiomyocytes exhibit capacitative calcium entry. *Am J Physiol Heart Circ Physiol* 2004;**286**:H1124–H1132.
- Collins HE, Zhu-Mauldin X, Marchase RB, Chatham JC. STIM1/*Orai1*-mediated SOCE: current perspectives and potential roles in cardiac function and pathology. *Am J Physiol Heart Circ Physiol* 2013;**305**:H446–H458.
- Lompre AM, Bernard L, Saliba Y, Aubart F, Fauconnier J, Hulot JS. STIM1 and *Orai1* in cardiac hypertrophy and vascular proliferative diseases. *Front Biosci (Schol Ed)* 2013;**5**:766–773.
- Roos J, DiGregorio PJ, Yeromin AV, Ohlsen K, Lioudyno M, Zhang S, Safrina O, Kozak JA, Wagner SL, Cahalan MD, Velicelebi G, Stauderman KA. STIM1, an essential and conserved component of store-operated  $\text{Ca}^{2+}$  channel function. *J Cell Biol* 2005;**169**:435–445.
- Liou J, Kim ML, Heo WD, Jones JT, Myers JW, Ferrell Jr JE, Meyer T. STIM is a  $\text{Ca}^{2+}$  sensor essential for  $\text{Ca}^{2+}$ -store-depletion-triggered  $\text{Ca}^{2+}$  influx. *Curr Biol* 2005;**15**:1235–1241.
- Zhang SL, Yu Y, Roos J, Kozak JA, Deerinck TJ, Ellisman MH, Stauderman KA, Cahalan MD. STIM1 is a  $\text{Ca}^{2+}$  sensor that activates CRAC channels and migrates from the  $\text{Ca}^{2+}$  store to the plasma membrane. *Nature* 2005;**437**:902–905.
- Soboloff J, Rothberg BS, Madesh M, Gill DL. STIM proteins: dynamic calcium signal transducers. *Nat Rev Mol Cell Biol* 2012;**13**:549–565.
- Hulot J-S, Fauconnier J, Ramanujam D, Chanaan A, Aubart F, Sassi Y, Merkle S, Cazorla O, Ouille A, Dupuis M, Hadri L, Jeong D, Muehlstedt S, Schmitt J, Braun A, Benard L, Saliba Y, Lagerbauer B, Nieswandt B, Lacampagne A, Hajjar RJ, Lompre A-M, Engelhardt S. Critical role for stromal interaction molecule 1 in cardiac hypertrophy. *Circulation* 2011;**124**:796–U109.
- Luo X, Hojavey B, Jiang N, Wang ZV, Tandan S, Rakalin A, Rothermel BA, Gillette TG, Hill JA. STIM1-dependent store-operated  $\text{Ca}^{2+}$ (+) entry is required for pathological cardiac hypertrophy. *J Mol Cell Cardiol* 2012;**52**:136–147.
- Ohba T, Watanabe H, Murakami M, Sato T, Ono K, Ito H. Essential role of STIM1 in the development of cardiomyocyte hypertrophy. *Biochem Biophys Res Commun* 2009;**389**:172–176.
- Voelkers M, Salz M, Herzog N, Frank D, Dolatabadi N, Frey N, Gude N, Friedrich O, Koch WJ, Katus HA, Sussman MA, Most P. *Orai1* and *Stim1* regulate normal and hypertrophic growth in cardiomyocytes. *J Mol Cell Cardiol* 2010;**48**:1329–1334.
- Collins HE, He L, Zou L, Qu J, Zhou L, Litovsky SH, Yang Q, Young ME, Marchase RB, Chatham JC. Stromal Interaction Molecule 1 is essential for normal cardiac homeostasis through modulation of ER and Mitochondrial function. *Am J Physiol Heart Circ Physiol* 2014;**15**:H1231–H1239.
- Mignen O, Shuttleworth TJ. I(ARC), a novel arachidonate-regulated, noncapacitative  $\text{Ca}^{2+}$  entry channel. *J Biol Chem* 2000;**275**:9114–9119.
- Mignen O, Thompson JL, Shuttleworth TJ. Reciprocal regulation of capacitative and arachidonate-regulated noncapacitative  $\text{Ca}^{2+}$  entry pathways. *J Biol Chem* 2001;**276**:35676–35683.
- Bisaillon JM, Motiani RK, Gonzalez-Cobos JC, Potier M, Halligan KE, Alzawhra WF, Barroso M, Singer HA, Jourdeuil D, Trebak M. Essential role for STIM1/*Orai1*-mediated calcium influx in PDGF-induced smooth muscle migration. *Am J Physiol Cell Physiol* 2010;**298**:C993–C1005.
- Potier M, Gonzalez JC, Motiani RK, Abdullaef IV, Bisaillon JM, Singer HA, Trebak M. Evidence for STIM1- and *Orai1*-dependent store-operated calcium influx through ICRAC in vascular smooth muscle cells: role in proliferation and migration. *Faseb J* 2009;**23**:2425–2437.
- Saliba Y, Mougenot N, Jacquet A, Atassi F, Hatem S, Fares N, Lompre AM. A new method of ultrasonic nonviral gene delivery to the adult myocardium. *J Mol Cell Cardiol* 2012;**53**:801–808.
- Huang J, van Breemen C, Kuo KH, Hove-Madsen L, Tibbits GF. Store-operated  $\text{Ca}^{2+}$  entry modulates sarcoplasmic reticulum  $\text{Ca}^{2+}$  loading in neonatal rabbit cardiac ventricular myocytes. *Am J Physiol Cell Physiol* 2006;**290**:C1572–C1582.
- Shuttleworth TJ. *Orai3*—the 'exceptional' *Orai*? *J Physiol* 2012;**590**:241–257.
- Wang P, Umeda PK, Sharifov OF, Halloran BA, Tabengwa E, Grenett HE, Urthaler F, Wolkowicz PE. Evidence that 2-aminoethoxydiphenyl borate provokes fibrillation in perfused rat hearts via voltage-independent calcium channels. *Eur J Pharmacol* 2012;**681**:60–67.
- Srikanth S, Gwack Y. Molecular Regulation of the Pore Component of CRAC Channels, *Orai1*. *Curr Top Membr* 2013;**71**:181–207.
- Park CY, Shcheglovitov A, Dolmetsch R. The CRAC channel activator STIM1 binds and inhibits L-type voltage-gated calcium channels. *Science* 2010;**330**:101–105.
- Wang Y, Deng X, Mancarella S, Hendron E, Eguchi S, Soboloff J, Tang XD, Gill DL. The calcium store sensor, STIM1, reciprocally controls *Orai* and  $\text{CaV}1.2$  channels. *Science* 2010;**330**:105–109.
- Jorgensen AO, Shen AC, Campbell KP. Ultrastructural localization of calsequestrin in adult rat atrial and ventricular muscle cells. *J Cell Biol* 1985;**101**:257–268.
- Horton JS, Buckley CL, Alvarez EM, Schorlemmer A, Stokes AJ. The calcium release-activated calcium channel *Orai1* represents a crucial component in hypertrophic compensation and the development of dilated cardiomyopathy. *Channels (Austin)* 2014;**8**:35–48.
- Hoth M, Niemeyer BA. The neglected CRAC proteins: *Orai2*, *Orai3*, and STIM2. *Curr Top Membr* 2013;**71**:237–271.
- Thompson JL, Shuttleworth TJ. Molecular basis of activation of the arachidonate-regulated  $\text{Ca}^{2+}$  (ARC) channel, a store-independent *Orai* channel, by plasma membrane STIM1. *J Physiol* 2013;**591**:3507–3523.
- Zhang X, Gonzalez-Cobos JC, Schindl R, Muik M, Ruhle B, Motiani RK, Bisaillon JM, Zhang W, Fahrner M, Barroso M, Matrougui K, Romanin C, Trebak M. Mechanisms of STIM1 activation of store-independent leukotriene C4-regulated  $\text{Ca}^{2+}$  channels. *Mol Cell Biol* 2013;**33**:3715–3723.

32. Putney JW. Alternative forms of the store-operated calcium entry mediators, STIM1 and Orai1. *Curr Top Membr* 2013;**71**:109–123.
33. Motiani RK, Abdullaev IF, Trebak M. A novel native store-operated calcium channel encoded by Orai3: selective requirement of Orai3 versus Orai1 in estrogen receptor-positive versus estrogen receptor-negative breast cancer cells. *J Biol Chem* 2010;**285**:19173–19183.
34. Faouzi M, Kischel P, Hague F, Ahidouch A, Benzerdjeb N, Sevestre H, Penner R, Ouadid-Ahidouch H. ORAI3 silencing alters cell proliferation and cell cycle progression via c-myc pathway in breast cancer cells. *Biochim Biophys Acta* 2013;**1833**:752–760.
35. Motiani RK, Zhang X, Harmon KE, Keller RS, Matrougui K, Bennett JA, Trebak M. Orai3 is an estrogen receptor alpha-regulated Ca(2)(+) channel that promotes tumorigenesis. *Faseb J* 2013;**27**:63–75.
36. Ay AS, Benzerdjeb N, Sevestre H, Ahidouch A, Ouadid-Ahidouch H. Orai3 constitutes a native store-operated calcium entry that regulates non small cell lung adenocarcinoma cell proliferation. *PLoS One* 2013;**8**:e72889.
37. Takemura H, Hughes AR, Thastrup O, Putney JW Jr. Activation of calcium entry by the tumor promoter thapsigargin in parotid acinar cells. Evidence that an intracellular calcium pool and not an inositol phosphate regulates calcium fluxes at the plasma membrane. *J Biol Chem* 1989;**264**:12266–12271.
38. Reibel DK, O'Rourke B, Foster KA, Hutchinson H, Uboh CE, Kent RL. Altered phospholipid metabolism in pressure-overload hypertrophied hearts. *Am J Physiol* 1986;**250**:H1–H6.
39. Mignen O, Thompson JL, Shuttleworth TJ. STIM1 regulates Ca<sup>2+</sup> entry via arachidonate-regulated Ca<sup>2+</sup>-selective (ARC) channels without store depletion or translocation to the plasma membrane. *J Physiol* 2007;**579**:703–715.
40. Shuttleworth TJ, Thompson JL, Mignen O. ARC channels: a novel pathway for receptor-activated calcium entry. *Physiology (Bethesda)* 2004;**19**:355–361.
41. Shuttleworth TJ, Thompson JL, Mignen O. STIM1 and the noncapacitative ARC channels. *Cell Calcium* 2007;**42**:183–191.
42. Mignen O, Thompson JL, Shuttleworth TJ. Both Orai1 and Orai3 are essential components of the arachidonate-regulated Ca<sup>2+</sup>-selective (ARC) channels. *J Physiol* 2008;**586**:185–195.
43. Gonzalez-Cobos JC, Zhang X, Zhang W, Ruhle B, Motiani RK, Schindl R, Muik M, Spinelli AM, Bissailon JM, Shinde AV, Fahrner M, Singer HA, Matrougui K, Barroso M, Romanin C, Trebak M. Store-independent Orai1/3 channels activated by intracrine leukotriene C4: role in neointimal hyperplasia. *Circ Res* 2013;**112**:1013–1025.
44. Zhang X, Zhang W, Gonzalez-Cobos JC, Jardin I, Romanin C, Matrougui K, Trebak M. Complex role of STIM1 in the activation of store-independent Orai1/3 channels. *J Gen Physiol* 2014;**143**:345–359.